Habilitation à Diriger des Recherches

Charles Dapogny

CNRS & Laboratoire Jean Kuntzmann, Université Grenoble Alpes, Grenoble, France

15th April, 2024

Foreword: Shape and topology optimization

- Shape optimization aims to minimize a function of the domain.
- Such problems can be traced back to the early human history...
- They are now as topical as ever, because of the needs to realize energy savings and to get free from fossile fuels.
- Despite its extensive academic and industrial treatments, the discipline keeps raising fascinating issues:
  - Develop mathematical tools, e.g. to measure the sensitivity of a quantity with respect to the domain.
  - Develop efficient numerical methods, that leverage recent achievements in scientific computing, machine learning, etc.
  - Address novel, challenging physical situations.
  - Propose realistic optimal design models, that notably take into account uncertainties and fabrication constraints.

Hooke's principle: "As hangs the flexible chain, so but inverted stands the rigid arch".

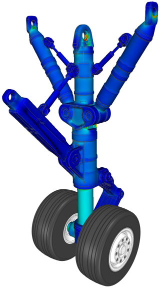

Optimized design of a landing gear (courtesy of `Ansys`*).*

Outline of the presentation

1. Motivation and background
   - Some basic material about shape optimization
   - Two recent numerical realizations

2. Towards realistic shape and topology optimization models
   - Shape optimization under uncertainties
   - Modeling fabrication constraints: the example of additive manufacturing

3. Asymptotic analysis for new types of shape variations
   - Optimization of boundary conditions
   - Topological ligaments

4. An ongoing project: Evolution of shapes via Laguerre diagrams

1. Motivation and background
   - Some basic material about shape optimization
   - Two recent numerical realizations
2. Towards realistic shape and topology optimization models
   - Shape optimization under uncertainties
   - Modeling fabrication constraints: the example of additive manufacturing
3. Asymptotic analysis for new types of shape variations
   - Optimization of boundary conditions
   - Topological ligaments
4. An ongoing project: Evolution of shapes via Laguerre diagrams

- A shape and topology optimization problem reads:

$$\boxed{\min_{\Omega} J(\Omega) \;\text{ s.t. }\; C(\Omega) \leq 0,}$$

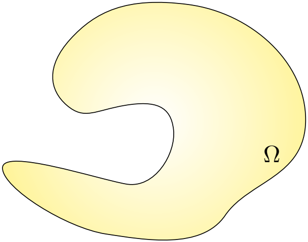

where

- The shape Ω is a bounded Lipschitz domain in $\mathbb{R}^d$;
- $J(\Omega)$ measures the physical performance of Ω;
- $C(\Omega)$ is a constraint functional.

- In applications, $J(\Omega)$ and $C(\Omega)$ depend on the physical behavior of Ω, via a state u_{Ω}, solution to a boundary value problem posed on Ω.

Shape and topology optimization in a nutshell (II)

Thermal (or electric) conduction

- Ω is a thermal cavity;
- $u_\Omega : \Omega \to \mathbb{R}$ is the temperature within Ω, solution to the conductivity equation;
- $J(\Omega)$ is the mean, or maximum temperature in Ω;
- $C(\Omega)$ is a constraint on the volume of Ω.

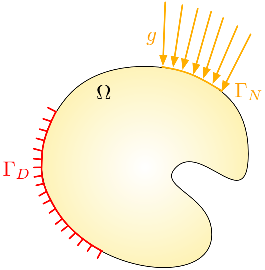

Structural mechanics

- Ω is a mechanical part;
- $u_\Omega : \Omega \to \mathbb{R}^d$ is the displacement of Ω, solution to the linear elasticity system;
- $J(\Omega)$ is the compliance of Ω;
- The constraint $C(\Omega)$ concerns the volume of Ω, its von Mises stress, etc.

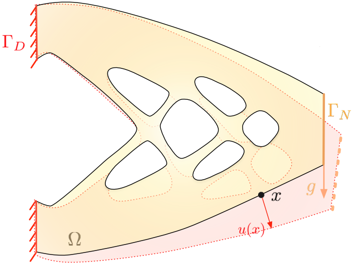

Shape and topology optimization in a nutshell (III)

- A shape and topology optimization problem reads:

$$\boxed{\min_{\Omega} J(\Omega) \;\text{ s.t. }\; C(\Omega) \leq 0,}$$

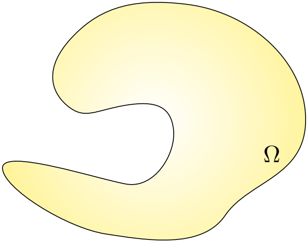

where

- The shape Ω is a bounded Lipschitz domain in $\mathbb{R}^d$;
- $J(\Omega)$ measures the physical performance of Ω;
- $C(\Omega)$ is a constraint functional.

- In applications, $J(\Omega)$ and $C(\Omega)$ depend on the physical behavior of Ω, via the solution u_Ω to a boundary value problem posed on Ω.

- The theoretical and numerical treatments of such problems rely on the "derivatives" of $\Omega \mapsto J(\Omega)$ and $\Omega \mapsto C(\Omega)$...

... a notion that can be understood in various ways.

Hadamard's boundary variation method.

Variations Ω of a shape are considered under the form

$$\Omega_\theta := (\mathrm{Id} + \theta)(\Omega),$$

where $\theta \in W^{1,\infty}(\mathbb{R}^d; \mathbb{R}^d)$ is a "small" vector field.

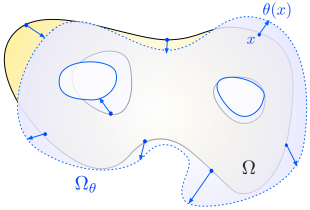

Definition 1.

The shape derivative *$J'(\Omega)(\theta)$ of a function $J(\Omega)$ is the Fréchet derivative of the underlying mapping $\theta \mapsto J(\Omega_\theta)$:*

$$J(\Omega_\theta) = J(\Omega) + J'(\Omega)(\theta) + \mathrm{o}(\theta).$$

A. Henrot and M. Pierre, *Shape Variation and Optimization*, EMS Tracts in Mathematics Vol. 28, 2018.

Different sensitivities with respect to the domain (II)

Nucleation of a tiny hole.

Variations of Ω are considered under the form

$$\Omega_{x_0,r} := \Omega \setminus \overline{B(x_0, r)},$$

where $x_0 \in \Omega$ and $r \ll 1$.

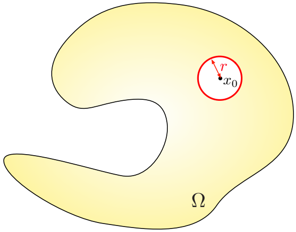

Definition 2.

A function $J(\Omega)$ has a topological derivative $\mathrm{d}J_T(\Omega)(x_0)$ at x_0 if the following expansion holds:

$$J(\Omega_{x_0,r}) = J(\Omega) + r^d \mathrm{d}J_T(\Omega)(x_0) + \mathrm{o}(r^d).$$

A. A. Novotny and J. Sokołowski, *Topological derivatives in shape optimization*, Springer Science & Business Media, 2012.

Different sensitivities with respect to the domain (III)

- The calculations of $J'(\Omega)(\theta)$ and $\mathrm{d}J_T(\Omega)(x)$ rely on the adjoint method.
- Their expressions depend on u_Ω and an adjoint state p_Ω.
- Assuming regularity of u_Ω and p_Ω, shape derivatives have the structure

$$J'(\Omega)(\theta) = \int_{\partial\Omega} v_\Omega(u_\Omega, p_\Omega)\, \theta \cdot n \,\mathrm{d}s,$$

  where $v_\Omega(u_\Omega, p_\Omega) : \partial\Omega \to \mathbb{R}$ has a closed form expression.
- A descent direction for $J(\Omega)$ is easily revealed from this structure:

$$\theta = -v_\Omega(u_\Omega, p_\Omega) n \text{ on } \partial\Omega \;\; \Rightarrow \;\; J'(\Omega)(\theta) < 0,$$

  i.e. "small deformations" of Ω according to θ decrease the value of $J(\Omega)$.
- Points $x \in \Omega$ s.t. $\mathrm{d}J_T(\Omega)(x) < 0$ indicate where it is beneficial to drill tiny holes.

J.-L. Lions, *Optimal control of systems governed by partial differential equations*, Grundlehren der mathematischen Wissenschaften, (1971), Springer-Verlag.

A steepest-descent strategy:

- At each iteration $n = 0, \ldots$, the shape Ω^n is equipped with a mesh $\mathcal{T}^n$.
- The finite element computations for u_{Ω^n} and p_{Ω^n} are performed on $\mathcal{T}^n$.
- A descent direction θ^n is obtained from $J'(\Omega^n)$, $C'(\Omega^n)$.
- The mesh updates $\mathcal{T}^n \to \mathcal{T}^{n+1}$ leverage a mesh evolution algorithm.
- Topological derivatives are periodically used to nucleate small holes inside Ω.

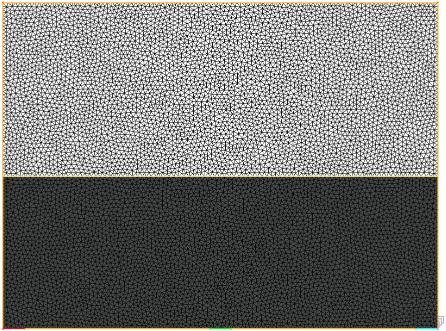

A word of advertisement

Mmg PLATFORM
Robust, Open-source & Multidisciplinary Software for Remeshing

Upgrade your meshes

The algorithms involved in this strategy are available as free, open-source codes.

- ISCDtoolbox: Algorithms for the level set method.

  `https://github.com/ISCDtoolbox`

- Mmg: A general purpose remeshing library.

  `https://www.mmgtools.org`

  `https://github.com/MmgTools/mmg`

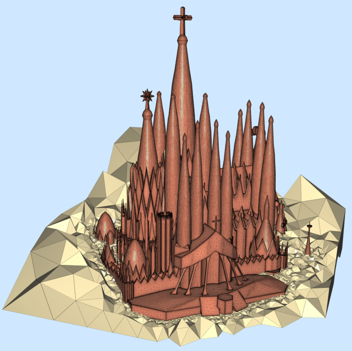

1. Motivation and background
   - Some basic material about shape optimization
   - Two recent numerical realizations
2. Towards realistic shape and topology optimization models
   - Shape optimization under uncertainties
   - Modeling fabrication constraints: the example of additive manufacturing
3. Asymptotic analysis for new types of shape variations
   - Optimization of boundary conditions
   - Topological ligaments
4. An ongoing project: Evolution of shapes via Laguerre diagrams

Optimization of a nanophotonic duplexer (I)

Joint work with A. Gliere, K. Hassan, N. Lebbe & E. Oudet

- Nanophotonic devices are the basic components of photonic integrated circuits.
- In these, light is transported by wave guides.
- The attached electric and magnetic fields are governed by Maxwell's equations.
- Duplexers steer incoming waves to different output channels, depending on their wavelength.
- The shape Ω of air inclusions in the Si core is optimized to achieve this effect.

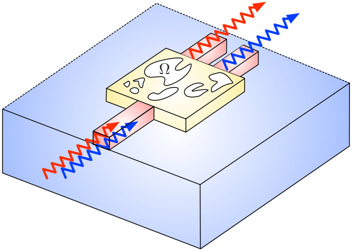

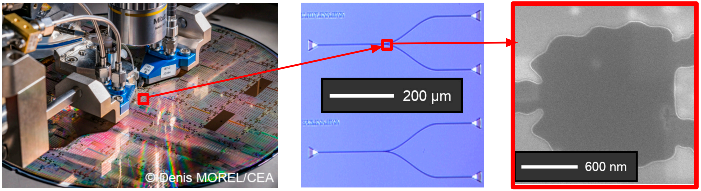

One nanophotonic component inside a complete photonic circuit.

Optimization of a nanophotonic duplexer (II)

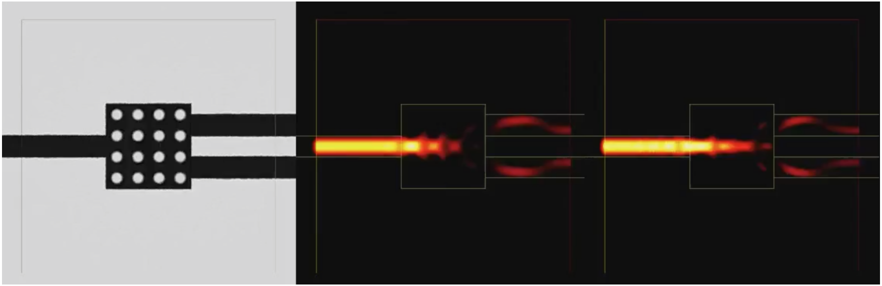

Optimization of the shape of a nanophotonic duplexer.

- A thermal chamber D is made of
  - A phase $\Omega_{f,\text{hot}}$ conveying a hot fluid;
  - A phase $\Omega_{f,\text{cold}}$ conveying a cold fluid;
  - A solid phase Ω_s.
- The Navier-Stokes equations are satisfied in $\Omega_{f,\text{hot}}$, $\Omega_{f,\text{cold}}$.
- The stationary heat equation accounts for the temperature diffusion within D.
- The heat transferred from $\Omega_{f,\text{hot}}$ to $\Omega_{f,\text{cold}}$ is maximized.
- A constraint is imposed on the minimal distance between $\Omega_{f,\text{hot}}$ and $\Omega_{f,\text{cold}}$:

$$d(\Omega_{f,\text{hot}}, \Omega_{f,\text{cold}}) \geq d_{\text{min}}.$$

- Volume and pressure drop constraints are added on $\Omega_{f,\text{hot}}$, $\Omega_{f,\text{cold}}$.

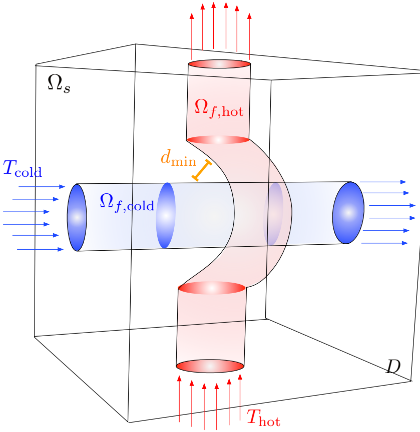

Optimization of the shape of a 3d heat exchanger (II)

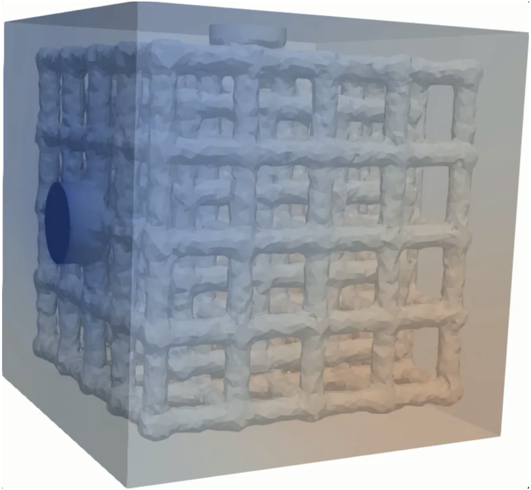

Optimization of the shape of a heat exchanger.

1. Motivation and background
   - Some basic material about shape optimization
   - Two recent numerical realizations

2. Towards realistic shape and topology optimization models
   - Shape optimization under uncertainties
   - Modeling fabrication constraints: the example of additive manufacturing

3. Asymptotic analysis for new types of shape variations
   - Optimization of boundary conditions
   - Topological ligaments

4. An ongoing project: Evolution of shapes via Laguerre diagrams

Robustness and fabrication constraints

Realistic optimal design studies are often expected to be aware of:

- Uncertainties about the parameters of the physical models.

  $\Rightarrow$ *We introduce various robust optimal design formulations, depending on the available information about uncertainties.*

- The constraints imposed on (the geometry of) the design by fabrication processes.

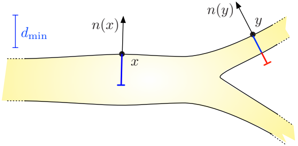

Thin parts are likely to break during cooling.

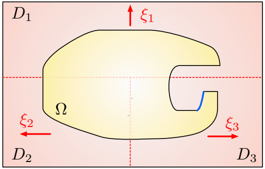

Molding processes make undercuts undesirable.

$\Rightarrow$ *We consider the overhang constraints imposed by the promising additive manufacturing technologies.*

K. Maute, *Topology optimization under uncertainty*, in Topology optimization in structural and continuum mechanics, (2014), pp. 457–471.

G. Michailidis, *Manufacturing constraints and multi-phase shape and topology optimization via a level-set method*, PhD thesis, Ecole Polytechnique, (2014).

1. Motivation and background
   - Some basic material about shape optimization
   - Two recent numerical realizations

2. Towards realistic shape and topology optimization models
   - Shape optimization under uncertainties
   - Modeling fabrication constraints: the example of additive manufacturing

3. Asymptotic analysis for new types of shape variations
   - Optimization of boundary conditions
   - Topological ligaments

4. An ongoing project: Evolution of shapes via Laguerre diagrams

Foreword: uncertainties in structural optimization

- A concrete shape optimization problem reads:

$$\boxed{\min_{\Omega} \mathcal{C}(\Omega, \xi) \quad (+ \text{ constraints}),}$$

where $\xi \in \Xi$ represents physical parameters.

- In structural mechanics, ξ may stand for:
  - The loads;
  - The material properties (e.g. Young's modulus);
  - The geometry of the system itself.
- In practice, these parameters are often uncertain:
  - They are identified via error-prone measurements,
  - They are altered with time (wear) and depend on the conditions of the ambient medium.
- The cost $\mathcal{C}(\Omega, \xi)$ (and the optimality of Ω) is usually very sensitive to even small perturbations of ξ.

$\Rightarrow$ Need to somehow anticipate uncertainties when designing and optimizing shapes.

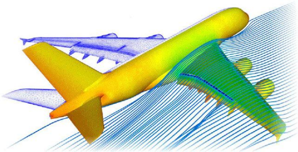

Drag on the wing of an aircraft (from *https://mximillinblogbll.blogspot.com)*

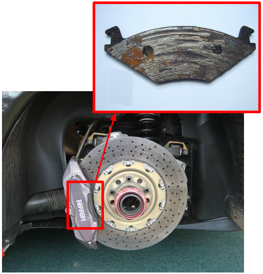

A worn out brake pad

- When nothing is known about ξ but a (small) bound m on its amplitude around a mean value ξ_0, worst-case formulations are considered:

$$\min_{\Omega} J_{\text{wc}}(\Omega), \text{ where } J_{\text{wc}}(\Omega) := \sup_{||\xi - \xi_0||_{\Xi} \leq m} \mathcal{C}(\Omega, \xi). \tag{WC}$$

- *Formal idea:* We linearize the cost $\mathcal{C}(\Omega, \xi)$ with respect to ξ:

$$\mathcal{C}(\Omega, \xi) \approx \mathcal{C}(\Omega, \xi_0) + \frac{\partial \mathcal{C}}{\partial \xi}(\Omega, \xi_0)(\xi) + \mathrm{o}(m),$$

  and then formally approximate

$$\begin{aligned} J_{\text{wc}}(\Omega) &\approx \sup_{||\xi - \xi_0||_{\Xi} \leq m} \left(\mathcal{C}(\Omega, \xi_0) + \tfrac{\partial \mathcal{C}}{\partial \xi}(\Omega, \xi_0)(\xi) \right) \\ &= \mathcal{C}(\Omega, \xi_0) + m \left|\left| \tfrac{\partial \mathcal{C}}{\partial \xi}(\Omega, \xi_0) \right|\right|_{\Xi^*}, \end{aligned}$$

  where $||\cdot||_{\Xi^*}$ is the dual norm of $||\cdot||_{\Xi}$.

- The resulting approximation of (WC) can be tackled by standard adjoint methods.

- Stochastic approaches assume a random distribution

$$\xi \equiv \xi(\omega),\ \ \omega \in \mathcal{O},\ \text{with law } \mathbb{P} \in \mathcal{P}(\Xi): \quad \forall A \subset \Xi,\ \ \mathbb{P}(A) = \int_{\mathcal{O}} \mathbb{1}_{\{\xi(\omega)\ \in A\}}\,\mathrm{d}\omega.$$

- The robust optimal design problem involves a moment of the cost $\mathcal{C}(\Omega, \xi)$, e.g.:

$$\min_{\Omega} J_{\text{mean}}(\Omega),\ \text{where } J_{\text{mean}}(\Omega) := \int_{\Xi} \mathcal{C}(\Omega, \xi)\,\mathrm{d}\mathbb{P}(\xi).$$

- We rely on the following assumptions about the uncertain parameters $\xi(\omega)$:

  1. $\xi(\omega)$ is "small", e.g. the norm $||\xi||_{L^p(\mathcal{O};\Xi)}$ is "small" for some $p \geq 1$.
  2. $\xi(\omega)$ is "finite-dimensional":

$$\xi(\omega) = \xi_0 + \sum_{i=1}^{N} \xi_i \alpha_i(\omega),$$

where $\xi_0, \xi_1, \ldots, \xi_N$ are deterministic parameters,

$$\int_{\mathcal{O}} \alpha_i(\omega)\,\mathrm{d}\omega = 0,\ \text{and } \int_{\mathcal{O}} \alpha_i(\omega)\alpha_j(\omega)\,\mathrm{d}\omega = \delta_{ij}, \quad i,j = 1, \ldots, N.$$

Such a reduced structure is obtained e.g. by a Karhunen-Loève expansion.

Various uncertainty paradigms: stochastic approaches (II)

- *Formal idea:* We linearize the cost $\mathcal{C}(\Omega,\xi)$ around the mean value ξ_0:

$$\mathcal{C}(\Omega,\xi) \approx \mathcal{C}(\Omega,\xi_0) + \frac{\partial \mathcal{C}}{\partial \xi}(\Omega,\xi_0)(\xi) + \frac{1}{2}\frac{\partial^2 \mathcal{C}}{\partial \xi^2}(\Omega,\xi_0)(\xi,\xi) + \mathrm{o}(||\xi-\xi_0||_{\Xi}^2).$$

- Injecting the structure of $\xi(\omega)$ and taking the mean value, it follows:

$$J_{\mathrm{mean}}(\Omega) \approx \mathcal{C}(\Omega,\xi_0) + \frac{1}{2}\sum_{i=1}^{N} \frac{\partial^2 \mathcal{C}}{\partial \xi^2}(\Omega,\xi_0)(\xi_i,\xi_i).$$

- This shape functional can be analyzed by standard adjoint techniques.
- A similar treatment yields an approximate variance or probability of failure:

$$J_{\mathrm{var}}(\Omega) := \int_{\Xi} \Big(\mathcal{C}(\Omega,\xi) - J_{\mathrm{mean}}(\Omega)\Big)^2 \, \mathrm{d}\xi \text{ and } J_{\mathrm{fail}}(\Omega) = \mathbb{P}\Big\{\xi \in \Xi,\ \ \mathcal{C}(\Omega,\xi) > \alpha\Big\},$$

where α is a safety threshold.

A numerical example

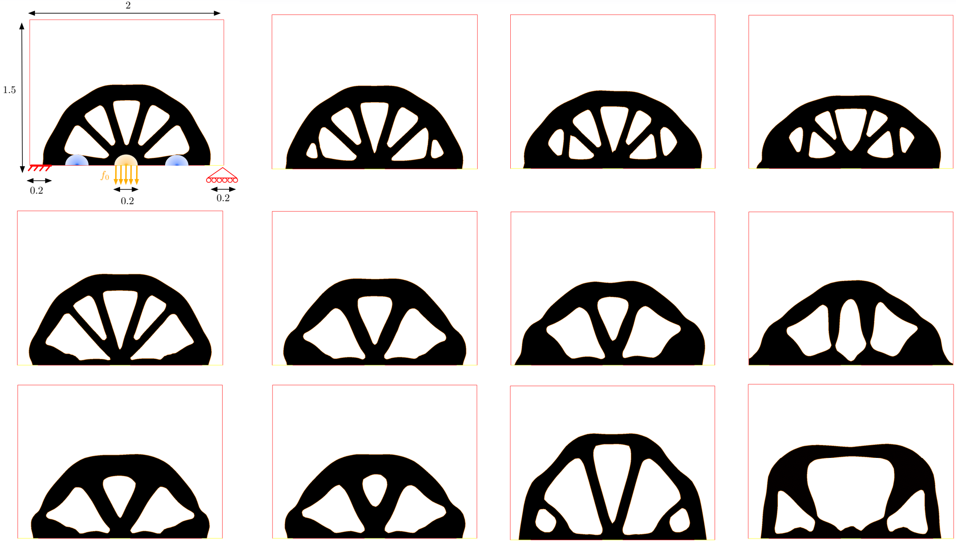

Optimized bridge considering (Top row) Random loads with the objective $J_{\mathrm{mean}}(\Omega)$ *and* $m = 1, 2, 5, 10$; *(middle row) Random loads with the objective* $J_{\mathrm{mean}}(\Omega) + \delta J_{\mathrm{var}}(\Omega)^{1/2}$ *and* $\delta = 3$, $m = 1, 2, 5, 10$; *(bottom row) The worst-case approach with* $m = 1, 2, 5, 10$.

Shortcomings of worst-case and stochastic approaches

Beyond computational aspects, neither of these paradigms is truly satisfactory.

- Worst-case approaches are pessimistic:

  Anticipating the (unlikely) worst-case scenario yields shapes with poor nominal performance.

- Stochastic approaches suffer from a major conceptual flaw:

  The law $\mathbb{P}$ of the uncertain parameters $\xi(\omega)$ is not known, and can at best be estimated from (a few) observed samples.

- Distributionally robust formulations only assume an estimate $\mathbb{P}$ of the law of the uncertain parameter ξ, that belongs to a compact set $\Xi \subset \mathbb{R}^k$.

- The worst mean value of $\mathcal{C}(\Omega, \xi)$ is minimized among laws $\mathbb{Q}$ that are "close" to $\mathbb{P}$:

$$\boxed{\min_{\Omega} J_{\mathrm{dr}}(\Omega), \text{ where } J_{\mathrm{dr}}(\Omega) = \sup_{\substack{\mathbb{Q} \in \mathcal{P}(\Xi) \\ d(\mathbb{Q},\mathbb{P}) \leq m}} \int_{\Xi} \mathcal{C}(\Omega, \xi) \, \mathrm{d}\mathbb{Q}(\xi).}$$

- The distance $d(\mathbb{Q}, \mathbb{P})$ between probability measures is the Wasserstein distance:

$$W(\mathbb{Q}, \mathbb{P}) = \inf_{\substack{\pi \in \mathcal{P}(\Xi \times \Xi) \\ \pi_{\mathbf{1}} = \mathbb{Q}, \ \pi_{\mathbf{2}} = \mathbb{P}}} \int_{\Xi \times \Xi} c(\xi, \zeta) \, \mathrm{d}\pi(\xi, \zeta),$$

where $c(\xi, \zeta) := |\xi - \zeta|^2$ is the ground cost of sending a unit of matter from ξ to ζ.

H. Rahimian and S. Mehrotra, *Distributionally robust optimization: A review*, arXiv preprint arXiv:1908.05659 (2019).

The Wasserstein distance (I)

- A coupling is a probability measure $\pi \in \mathcal{P}(\Xi \times \Xi)$.
- The marginals $\pi_1, \pi_2 \in \mathcal{P}(\Xi)$ of $\pi \in \mathcal{P}(\Xi \times \Xi)$ are defined by:

$$\forall \varphi \in \mathcal{C}(\Xi), \quad \int_{\Xi \times \Xi} \varphi(\xi) \mathrm{d}\pi(\xi, \zeta) = \int_{\Xi} \varphi(\xi)\, \mathrm{d}\pi_1(\xi), \text{ and}$$

$$\int_{\Xi \times \Xi} \varphi(\zeta) \mathrm{d}\pi(\xi, \zeta) = \int_{\Xi} \varphi(\zeta)\, \mathrm{d}\pi_2(\zeta).$$

- *Interpretation:* $\pi(\xi, \zeta) \approx$ amount of mass of $\mathbb{P}$ at ζ coming from mass at ξ in $\mathbb{Q}$.
- $W(\mathbb{Q}, \mathbb{P})$ thus measures the optimal way to transport the mass from $\mathbb{Q}$ to $\mathbb{P}$.
- It is a "geometric" quantity to appraise the difference between $\mathbb{P}$ and $\mathbb{Q}$.

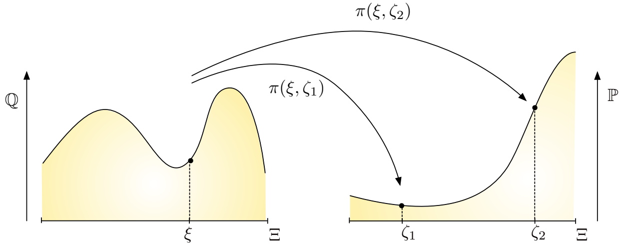

The Wasserstein distance (II)

The blurred, entropy-regularized Wasserstein distance is used:

$$W_\varepsilon(\mathbb{Q},\mathbb{P}) = \inf_{\substack{\pi\in\mathcal{P}(\Xi\times\Xi)\\ \pi_1=\mathbb{Q},\ \pi_2=\mathbb{P}}} \left(\int_{\Xi\times\Xi} c(\xi,\zeta)\mathrm{d}\pi(\xi,\zeta) + \varepsilon H(\pi) \right),$$

where the entropy $H(\pi)$ of a coupling π is:

$$H(\pi) = \begin{cases} \int_{\Xi\times\Xi} \log\left(\frac{\mathrm{d}\pi}{\mathrm{d}\pi_0}\right)\mathrm{d}\pi & \text{if } \pi \text{ is a.c. w.r.t. } \pi_0 \\ +\infty & \text{otherwise,} \end{cases}$$

and the reference coupling π_0 is:

$$\pi_0(\xi,\zeta) = \mathbb{P}(\xi)\mathrm{d}\nu_\xi(\zeta), \quad \text{with} \quad \mathrm{d}\nu_\xi(\zeta) := \alpha_\xi e^{-\frac{c(\xi,\zeta)}{2\sigma}} \mathbb{1}_\Xi(\zeta)\mathrm{d}\zeta,$$

for some $\sigma > 0$ and a normalization factor α_ξ, i.e.

π_0 "spreads" the mass of $\mathbb{P}$ at ξ over a characteristic length σ.

G. Peyré and M. Cuturi, *Computational optimal transport: With applications to data science*, Foundations and Trends in Machine Learning, 11 (2019), pp. 355–607.
F. Santambrogio, *Optimal transport for applied mathematicians*, Birkäuser, 2015.

Ongoing work: distributionally robust formulations (III)

We use the following result from convex duality.

Theorem 1.

Let $f : \Xi \to \mathbb{R}$ be a continuous function, and $\mathbb{P} \in \mathcal{P}(\Xi)$ be a probability measure. Then, for any $m > 0$ and for σ small enough,

$$\sup_{W_\varepsilon(\mathbb{P},\mathbb{Q}) \leq m} \int_\Xi f(\zeta)\, \mathrm{d}\mathbb{Q}(\zeta) = \inf_{\lambda \geq 0} \left\{ \lambda m + \lambda \varepsilon \int_\Xi \log \left(\int_\Xi e^{\frac{f(\zeta) - \lambda c(\xi,\zeta)}{\lambda \varepsilon}} \mathrm{d}\nu_\xi(\zeta) \right) \mathrm{d}\mathbb{P}(\xi) \right\}.$$

The distributionally robust problem has a tractable reformulation:

$$\min_{\Omega, \lambda \geq 0} \mathcal{D}(\Omega, \lambda), \text{ where}$$

$$\mathcal{D}(\Omega, \lambda) := \lambda m + \lambda \varepsilon \int_\Xi \log \left(\int_\Xi e^{\frac{\mathcal{C}(\Omega,\zeta) - \lambda c(\xi,\zeta)}{\lambda \varepsilon}} \mathrm{d}\nu_\xi(\zeta) \right) \mathrm{d}\mathbb{P}(\xi).$$

W. Azizian, F. Iutzeler and J. Malick, *Regularization for Wasserstein distributionally robust optimization*, ESAIM: Control, Optimisation and Calculus of Variations, (2023), 29, 33.

Ongoing work: distributionally robust formulations

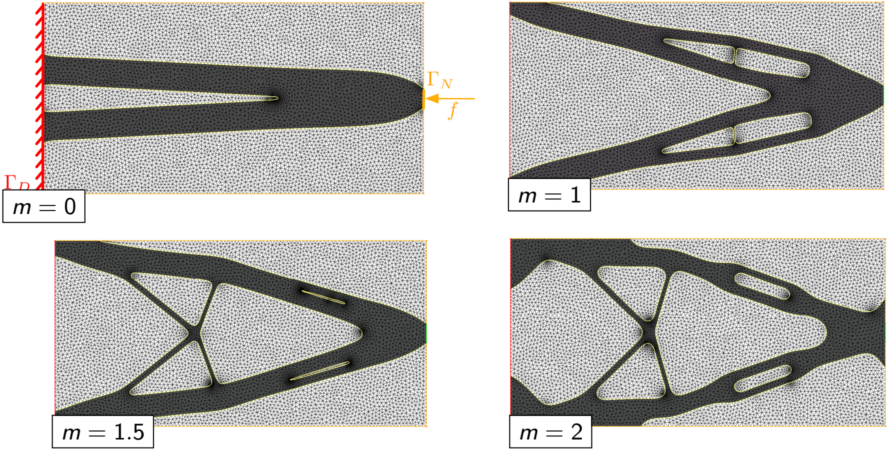

Distributionally robust shapes of the cantilever for various values of m*.*

Additive manufacturing in a nutshell

- Additive manufacturing technologies (a.k.a. 3d printing) proceed by decomposing the shape into horizontal layers, which are assembled one on top of the other.

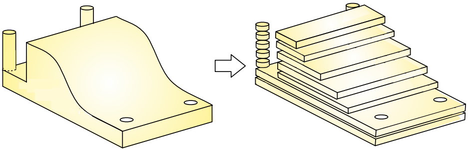

- 3d printing technologies differ on how each individual layer is fabricated.

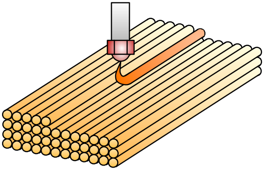

Material extrusion methods (e.g. FDM), used to process plastic (ABS), act by deposition of a molten filament.

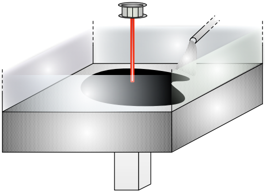

Powder bed fusion methods (e.g. EBM, SLS) process metals; metallic powder is spread within the build chamber, and a laser binds the grains together.

- 3d printing techniques can allegedly process arbitrarily complex shapes.

The overhang issue

All additive manufacturing technologies experience trouble when assembling shapes with large overhangs, i.e. regions hanging over void.

- In the case of FDM processes, this amounts to assembling over void.
- In powder-bed methods, these regions cannot efficiently evacuate heat, inducing residual stress and warpage during cooling.
- A common, but cumbersome strategy to handle overhangs is to erect a sacrificial scaffold structure alongside the construction of the shape.

$\Rightarrow$ Desire to add an overhang constraint $P(\Omega)$ in the optimal design problem.

(Left) Warpage caused by residual constraints in EBM (from [PoFarCoMa]); (right) Supporting scaffold structure (from `https://filament2print.com`).

Insufficiency of geometric constraints: the "dripping effect"

- **Geometric attempt:** $P(\Omega)$ penalizes regions of $\partial\Omega$ "close" from horizontal, e.g.

$$P(\Omega) = \int_{\partial\Omega} \varphi(n_\Omega)\,\mathrm{d}s, \text{ where } \varphi : \mathbb{R}^d \to \mathbb{R} \text{ is given.}$$

- The results are undesirable: such functions induce "many" local minima", where the constraint is satisfied "almost everywhere".

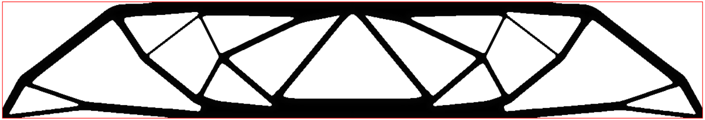

Optimized shape of a 2d MBB Beam (without manufacturing constraint).

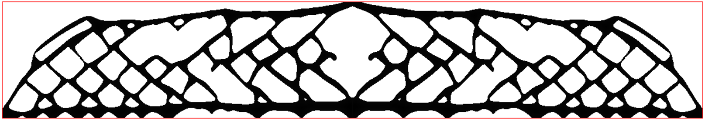

Optimized shape accommodating a geometric constraint, which is fulfilled "almost everywhere"!

We rely on a mechanical constraint $P(\Omega)$ which appraises the physical behavior of the shape at each stage of its construction.

- Ω is enclosed in the build chamber $D = S \times (0, H)$, where $S \subset \mathbb{R}^{d-1}$,
- $\Omega_h := \{x = (x_1, ..., x_d) \in \Omega,\ x_d < h\}$ is the intermediate shape at height h.
- The boundary $\partial\Omega_h$ is decomposed as $\partial\Omega_h = \Gamma_0 \cup \Gamma_h^u \cup \Gamma_h^l$, where

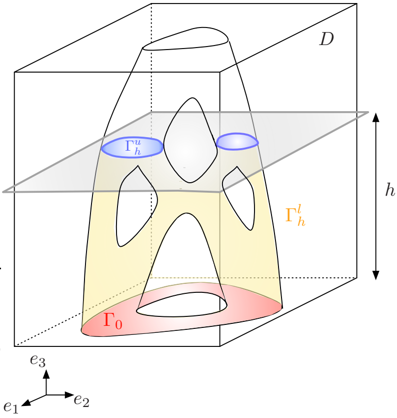

- $\Gamma_0 = \{x \in \partial\Omega_h,\ \ x_d = 0\}$ is the contact region between Ω_h and the build table,
- $\Gamma_h^u = \{x \in \partial\Omega_h,\ \ x_d = h\}$ is the upper side of Ω_h,
- $\Gamma_h^l = \partial\Omega_h \setminus (\overline{\Gamma_0} \cup \overline{\Gamma_h^u})$ is the lateral surface.

A mechanical constraint for overhang features (II)

- Each intermediate shape Ω_h is only subjected to gravity effects $g \in H^1(\mathbb{R}^d)^d$.
- The displacement $u^c_{\Omega_h}$ of Ω_h during construction ($\neq$ final use) satisfies:

$$\begin{cases} -\mathrm{div}(Ae(u_{\Omega^c_h})) = g & \text{in } \Omega_h, \\ u^c_{\Omega_h} = 0 & \text{on } \Gamma_0, \\ Ae(u^c_{\Omega_h})n = 0 & \text{on } \Gamma^l_h \cup \Gamma^u_h. \end{cases}$$

- The self-weight of each intermediate shape Ω_h is:

$$c_{\Omega_h} := \int_{\Omega_h} Ae(u^c_{\Omega_h}) : e(u^c_{\Omega_h})\,\mathrm{d}x = \int_{\Omega_h} g \cdot u^c_{\Omega_h}\,\mathrm{d}x.$$

- The manufacturing compliance of Ω aggregates the self weights of its intermediate shapes:

$$P_{\mathrm{sw}}(\Omega) = \int_0^H j(c_{\Omega_h})\,\mathrm{d}h,$$

where $j : \mathbb{R} \to \mathbb{R}$ is a smooth function.

A mechanical constraint for overhang features (III)

- The shape derivative of the constraint $P_{\mathrm{sw}}(\Omega)$ can be calculated.

- Other models may be used for the physical behavior of intermediate shapes Ω_h, e.g.
  - The problem for the displacement $u^c_{\Omega_h}$ of Ω_h could be replaced by:

$$\left\{ \begin{array}{cl} -\mathrm{div}(Ae(u^a_{\Omega_h})) = g_h & \text{in } \Omega_h, \\ u^a_{\Omega_h} = 0 & \text{on } \Gamma_0, \\ Ae(u^a_{\Omega_h})n = 0 & \text{on } \Gamma^l_h, \\ Ae(u^a_{\Omega_h})n = 0 & \text{on } \Gamma^u_h, \end{array} \right. \quad \text{where } g_h(x) = \left\{ \begin{array}{ll} g & \text{if } \; x_d \in (h-\delta, h), \\ 0 & \text{otherwise,} \end{array} \right.$$

    is the force applied by the printing tool on the upper side of Ω_h.

  - In [AlJak], the constraint $P(\Omega)$ involves the solution T_{Ω_h} to a thermal cooling problem posed on Ω_h, to model residual stresses in the final shape Ω.

A mechanical constraint for overhang features (IV): example

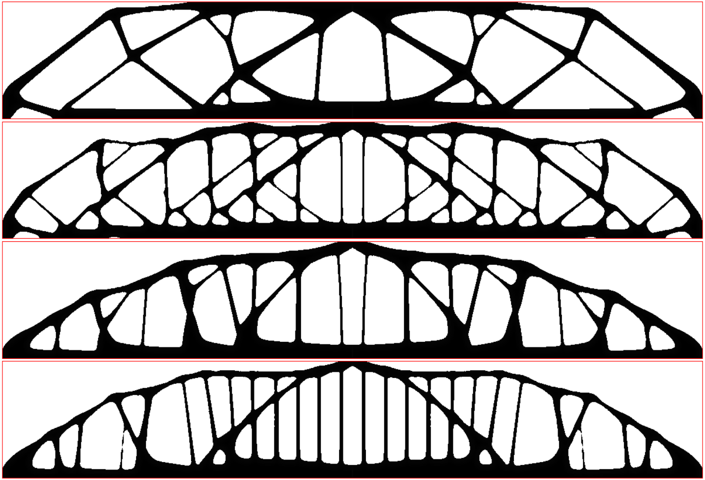

Optimized 2d MBB Beams obtained using the modified manufacturing compliance $P_{\mathrm{af}}(\Omega)$ and parameters (from top to bottom) $\alpha_c = 0.30$, $\alpha_c = 0.10$, $\alpha_c = 0.05$, and $\alpha_c = 0.03$.

1. Motivation and background
   - Some basic material about shape optimization
   - Two recent numerical realizations

2. Towards realistic shape and topology optimization models
   - Shape optimization under uncertainties
   - Modeling fabrication constraints: the example of additive manufacturing

3. Asymptotic analysis for new types of shape variations
   - Optimization of boundary conditions
   - Topological ligaments

4. An ongoing project: Evolution of shapes via Laguerre diagrams

Asymptotic analysis: foreword

Asymptotic analysis generally deals with the effect of "small perturbations" on the solution to a boundary value problem, indexed by $\varepsilon \ll 1$. They may be

- Regularized versions of a singular boundary value problem,
- Singular perturbations of "smooth" partial differential equations.

A representative issue of the second category is the analysis of the effect of small inhomogeneities within a background medium.

Small inhomogeneities in a background medium (I)

- Background situation: u_0 is the potential associated to a smooth conductivity γ_0 within $D \subset \mathbb{R}^d$:

$$\begin{cases} -\text{div}(\gamma_0 \nabla u_0) = f & \text{in } D, \\ u_0 = 0 & \text{on } \partial D. \end{cases}$$

- Perturbed situation: γ_0 is replaced by another smooth conductivity γ_1 inside a "small" subset $\omega_\varepsilon \Subset D$:

$$\begin{cases} -\text{div}(\gamma_\varepsilon \nabla u_\varepsilon) = f & \text{in } D, \\ u_\varepsilon = 0 & \text{on } \partial D, \end{cases}$$

where $\gamma_\varepsilon(x) := \begin{cases} \gamma_1(x) & \text{if } x \in \omega_\varepsilon, \\ \gamma_0(x) & \text{otherwise.} \end{cases}$

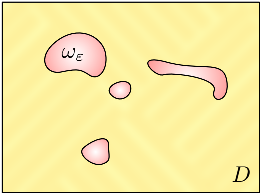

What is the behavior of the perturbed potential u_ε by the presence of inclusions ω_ε of conductivity γ_1 in the background medium?

Small inhomogeneities in a background medium (II)

- A general representation formula for u_ε is (up to a subsequence of the ε):

$$\boxed{u_\varepsilon(x) = u_0(x) + |\omega_\varepsilon| \int_D \mathcal{M}(y) \nabla u_0(y) \cdot \nabla_y N(x,y) \, \mathrm{d}\mu(y) + \mathrm{o}(|\omega_\varepsilon|),}$$

where

- μ is a positive measure indicating the "limiting position" of the sets ω_ε;
- The polarization tensor $\mathcal{M}(y)$ encodes the limiting "near field" u_ε inside ω_ε;
- $N(x,y)$ is the Green's function for the background problem.

- Under "mild" conditions, the quantity $J(u_\varepsilon) := \int_D j(u_\varepsilon) \, \mathrm{d}x$ has the expansion:

$$J(u_\varepsilon) = J(u_0) - |\omega_\varepsilon| \int_D \mathcal{M}(y) \nabla u_0(y) \cdot \nabla p_0(y) \, \mathrm{d}\mu(y) + \mathrm{o}(|\omega_\varepsilon|),$$

where the adjoint state p_0 is defined by $\left\{ \begin{array}{cl} -\mathrm{div}(\gamma_0 \nabla p_0) = -j'(u_0) & \text{in } D, \\ p_0 = 0 & \text{on } \partial D. \end{array} \right.$

Y. Capdeboscq and M. S. Vogelius, *A general representation formula for boundary voltage perturbations caused by internal conductivity inhomogeneities of low volume fraction*, ESAIM: M2AN, 37 (2003), pp. 159–173.

Small inhomogeneities in a background medium (III)

Diametrically small inhomogeneities

$$\omega_\varepsilon = x_0 + \varepsilon\omega,$$

where $\omega \Subset \mathbb{R}^d$ is a given bounded subset.

- μ is a multiple of δ_{x_0},
- $\mathcal{M}$ involves the solution to an exterior problem, posed on ω and $\mathbb{R}^d \setminus \overline{\omega}$.

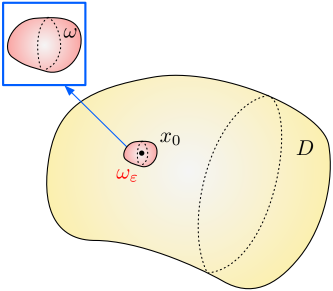

A 3d diametrically small inhomogeneity

Small tubular inhomogeneities

$$\omega_{\sigma,\varepsilon} = \left\{ x \in \mathbb{R}^d, \;\; d(x,\sigma) < \varepsilon \right\},$$

where $\sigma \Subset D$ is an (open or closed) curve in $\mathbb{R}^d$.

- μ is an integration measure on σ,
- $\mathcal{M}$ is diagonal in a local basis $(\tau, n_1, \dots, n_{d-1})$ attached to σ.
- These have been seldom considered [BCGF, CGK].

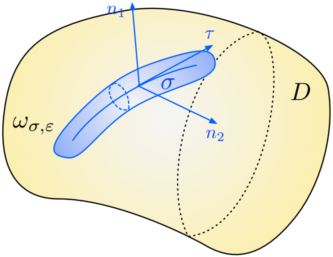

A 3d tubular inhomogeneitiy.

Foreword

We investigate two forays of asymptotic analysis in shape and topology optimization.

Optimization of the regions supporting boundary conditions

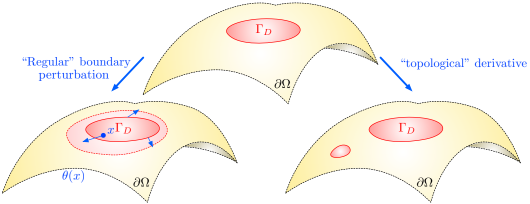

Optimization of the topology of shapes by the graft of thin ligaments

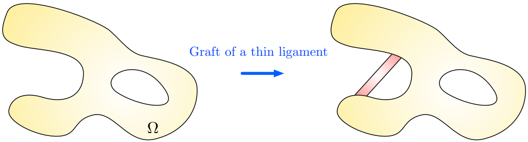

1. Motivation and background
   - Some basic material about shape optimization
   - Two recent numerical realizations
2. Towards realistic shape and topology optimization models
   - Shape optimization under uncertainties
   - Modeling fabrication constraints: the example of additive manufacturing
3. Asymptotic analysis for new types of shape variations
   - Optimization of boundary conditions
   - Topological ligaments
4. An ongoing project: Evolution of shapes via Laguerre diagrams

Optimization of boundary conditions: examples

Thermal conduction

- The temperature $u_\Omega : \Omega \to \mathbb{R}$ inside Ω is the solution to the conductivity equation;
- Dirichlet b.c. account for a known profile;
- Neumann b.c. represent an imposed heat flux.

Structure mechanics

- The displacement $u_\Omega : \Omega \to \mathbb{R}^d$ of Ω is solution to the linear elasticity system;
- Ω is attached at the regions equipped with homogeneous Dirichlet b.c. ;
- Neumann b.c. represent applied surface loads.

Optimization of the screws of a mandibular prosthesis [LaBa].

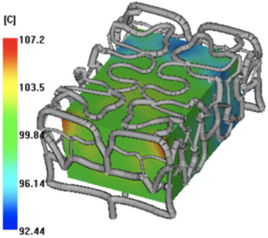

Optimized cooling process for a structure produced by molding [WeWuShi].

A model situation (I)

- The considered shapes Ω are smooth, bounded domains in $\mathbb{R}^d$, with boundaries:

$$\partial\Omega = \overline{\Gamma_D} \cup \overline{\Gamma_N} \cup \overline{\Gamma}.$$

- We assume that $\overline{\Gamma_D} \cap \overline{\Gamma_N} = \emptyset$ and denote

$$\Sigma_D = \partial\Gamma_D, \text{ and } \Sigma_N = \partial\Gamma_N.$$

- The behavior of Ω is dictated by the solution $u_\Omega \in H^1(\Omega)$ to the conductivity equation:

$$\begin{cases} -\mathrm{div}(\gamma\nabla u_\Omega) = f & \text{in } \Omega, \\ u_\Omega = 0 & \text{on } \Gamma_D, \\ \gamma\frac{\partial u_\Omega}{\partial n} = 0 & \text{on } \Gamma, \\ \gamma\frac{\partial u_\Omega}{\partial n} = g & \text{on } \Gamma_N, \end{cases}$$

where
- γ is the conductivity of the medium,
- $f \in L^2(\Omega)$ is a source (or a sink),
- $g \in L^2(\Gamma_N)$ is a heat flux.

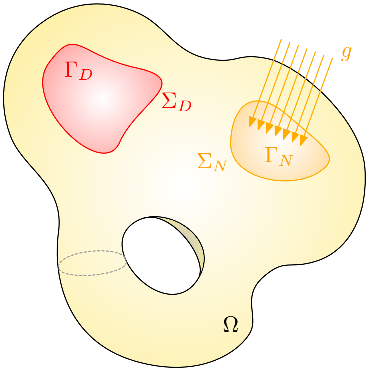

A model situation (II)

- We consider a shape functional of the form

$$J(\Omega) := \int_\Omega j(u_\Omega)\,\mathrm{d}x, \text{ for some smooth } \; j : \mathbb{R} \to \mathbb{R},$$

  which depends on Ω, but also on the repartition of Γ_D, Γ_N and Γ on $\partial\Omega$.

- We aim to

  1. Calculate the shape derivative $J'(\Omega)(\theta)$ when deformations θ do not vanish near Γ_D.
  2. Calculate "topological derivatives", measuring the sensitivity of $J(\Omega)$ to the insertion of a small Dirichlet subset ω_ε inside Γ.

- The presented methods can be generalized to

  - Other types of regions (derivative of $\Gamma_N \mapsto J(\Omega)$, transitions between homogeneous / inhomogeneous Dirichlet conditions, etc.),
  - Other physical contexts (linear elasticity, acoustics, etc).

$J'(\Omega)(\theta)$ has an intricate expression because of the limited regularity of u_Ω near Σ_D:

- There is a neighborhood W of each $x \in \overline{\Omega} \setminus (\Sigma_D \cup \Sigma_N)$ s.t. u_Ω is smooth in $\Omega \cap W$.
- u_Ω is weakly singular near Σ_D (i.e. $H^{3/2-\eta}$ for all $\eta > 0$).

Illustration: In 2d, assuming a flat boundary $\partial\Omega$ near $\Sigma_D = \{s_0, s_1\}$

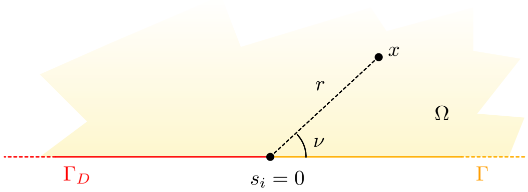

$u_\Omega = u_r^i + c^i S^i$ near s_i, where

- u_r^i belongs to $H^2(\Omega \cap V)$,
- c_i is a scalar coefficient,
- $S^i(r,\nu) = r^{\frac{1}{2}} \cos\left(\frac{\nu}{2}\right)$.

P. Grisvard, *Elliptic problems in nonsmooth domains*, SIAM, (2011).

Approximation of the optimization problem (I)

- We introduce a regularized problem:

$$\begin{cases} -\mathrm{div}(\gamma \nabla u_{\Omega,\varepsilon}) = f & \text{in } \Omega, \\ \gamma \dfrac{\partial u_{\Omega,\varepsilon}}{\partial n} + h_\varepsilon u_{\Omega,\varepsilon} = 0 & \text{on } \Gamma \cup \Gamma_D, \\ \gamma \dfrac{\partial u_{\Omega,\varepsilon}}{\partial n} = g & \text{on } \Gamma_N. \end{cases}$$

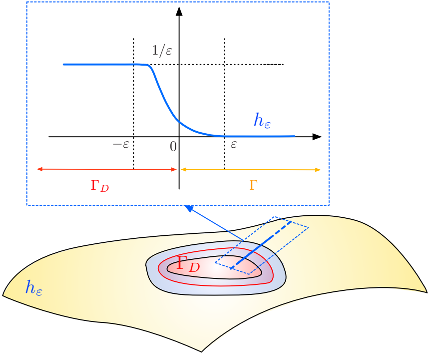

- $h_\varepsilon(x) := \frac{1}{\varepsilon} h\left(\frac{d^{\partial\Omega}_{\Gamma_D}(x)}{\varepsilon}\right)$ is made from:

  - The geodesic signed distance $d^{\partial\Omega}_{\Gamma_D}$ to Γ_D,
  - A smooth profile $h : \mathbb{R} \to \mathbb{R}$ such that:

$$0 \leq h \leq 1, \quad \begin{cases} h \equiv 1 & \text{on } (-\infty, -1], \\ h(0) > 0, & \\ h \equiv 0 & \text{on } [1, \infty). \end{cases}$$

- Intuitively,
  - $h_\varepsilon = 0$ "well inside" Γ ($\approx$ homogeneous Neumann b.c.),
  - $h_\varepsilon = \frac{1}{\varepsilon} \approx \infty$ in Γ_D ($\approx$ homogeneous Dirichlet b.c.).

- For a fixed $\varepsilon > 0$, standard elliptic regularity implies that $u_{\Omega,\varepsilon}$ is smooth on $\overline{\Omega}$.

Approximation of the optimization problem (II)

- This approximation gives rises to an approximate shape functional:

$$J_\varepsilon(\Omega) = \int_\Omega j(u_{\Omega,\varepsilon})\,\mathrm{d}x.$$

- Its shape derivative can be calculated by standard adjoint methods and is simple to handle in algorithms.
- Under "mild" assumptions, the following convergence results hold true:
  - The function $u_{\Omega,\varepsilon}$ converges to u_Ω strongly in $H^1(\Omega)$: for any $0 < s < \frac{1}{4}$,

$$||u_{\Omega,\varepsilon} - u_\Omega||_{H^1(\Omega)} \leq C_s \varepsilon^s ||f||_{L^2(\Omega)}.$$

  - The approximate functional $J_\varepsilon(\Omega)$ converges to its exact counterpart $J(\Omega)$.
  - The approximate shape derivative $J'_\varepsilon(\Omega)$ converges to the exact one $J'(\Omega)$:

$$\sup_{||\theta||_{W^{1,\infty}(\mathbb{R}^d,\mathbb{R}^d)} \leq 1} |J'_\varepsilon(\Omega)(\theta) - J'(\Omega)(\theta)| \xrightarrow{\varepsilon \to 0} 0.$$

- Let $\omega_\varepsilon \subset \Gamma$ be the surface disk with center x_0 and radius ε.
- The background and perturbed potentials u_Ω and u_ε are the $H^1(\Omega)$ solutions to:

$$\left\{\begin{array}{rll} -\mathrm{div}(\gamma\nabla u_\Omega) = f & \text{in } \Omega, \\ u_\Omega = 0 & \text{on } \Gamma_D, \\ \gamma\frac{\partial u_\Omega}{\partial n} = 0 & \text{on } \Gamma, \\ \gamma\frac{\partial u_\Omega}{\partial n} = g & \text{on } \Gamma_N. \end{array}\right.$$

$$\left\{\begin{array}{rll} -\mathrm{div}(\gamma\nabla u_\varepsilon) = f & \text{in } \Omega, \\ u_\varepsilon = 0 & \text{on } \Gamma_D \cup \omega_\varepsilon, \\ \gamma\frac{\partial u_\varepsilon}{\partial n} = 0 & \text{on } \Gamma \setminus \overline{\omega_\varepsilon}, \\ \gamma\frac{\partial u_\varepsilon}{\partial n} = g & \text{on } \Gamma_N. \end{array}\right.$$

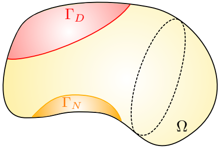

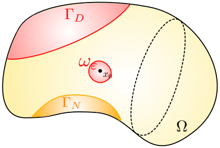

Theorem 2.

The following asymptotic expansion holds at any point $x \in \overline{\Omega}$, $x \notin \Sigma \cup \{x_0\}$:

$$u_\varepsilon(x) = \left\{\begin{array}{ll} u_\Omega(x) - \frac{\pi}{|\log\varepsilon|}\gamma(x_0)u_\Omega(x_0)N(x,x_0) + \mathrm{o}\left(\frac{1}{|\log\varepsilon|}\right) & \text{if } d = 2, \\ u_\Omega(x) - 4\varepsilon\gamma(x_0)u_\Omega(x_0)N(x,x_0) & \text{if } d = 3. \end{array}\right.$$

The corresponding perturbed version of $J(\Omega)$ reads:

$$J(\varepsilon) = \int_\Omega j(u_\varepsilon)\, \mathrm{d}x.$$

Corollary 3.

The function $J(\varepsilon)$ has the following asymptotic expansion at 0:

$$J(\varepsilon) = \begin{cases} J(0) + \dfrac{\pi}{|\log \varepsilon|}\gamma(x_0)u_\Omega(x_0)p_\Omega(x_0) + \mathrm{o}\left(\dfrac{1}{|\log \varepsilon|}\right) & \text{if } d = 2, \\ J(0) + 4\varepsilon\gamma(x_0)u_\Omega(x_0)p_\Omega(x_0) + \mathrm{o}(\varepsilon) & \text{if } d = 3, \end{cases}$$

where p_Ω is the unique solution in $H^1(\Omega)$ to the boundary value problem:

$$\begin{cases} -\mathrm{div}(\gamma\nabla p_\Omega) = -j'(u_\Omega) & \text{in } \Omega, \\ p_\Omega = 0 & \text{on } \Gamma_D, \\ \gamma\frac{\partial p_\Omega}{\partial n} = 0 & \text{on } \Gamma_N. \end{cases}$$

$\Rightarrow$ *The negativity of the first non-trivial term indicates where to add Dirichlet b.c.*

Example: Optimization of a micro-osmotic mixer (I)

- Electro-osmotic mixers achieve the mixture of two fluids inside a device Ω by maximizing the electric field induced by electrodes on $\partial\Omega$.
- The boundary of Ω is decomposed as:

$$\partial\Omega = \overline{\Gamma_C} \cup \overline{\Gamma_A} \cup \overline{\Gamma},$$

where
- Γ_C is the cathode,
- Γ_A is the anode,
- Ω is insulated on Γ.

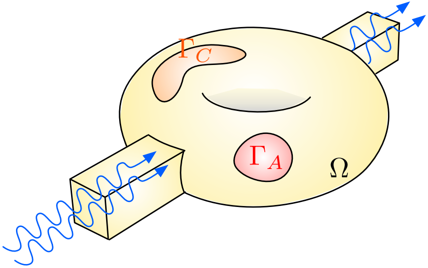

- The potential inside Ω is the solution to:

$$\begin{cases} -\text{div}(\gamma \nabla u_\Omega) = 0 & \text{in } \Omega, \\ u_\Omega = 0 & \text{on } \Gamma_C, \\ u_\Omega = u_{\text{in}} & \text{on } \Gamma_A, \\ \gamma \frac{\partial u_\Omega}{\partial n} = 0 & \text{on } \Gamma. \end{cases}$$

- We aim to maximize the electric power inside Ω with respect to Γ_A and Γ_C:

$$J(\Omega) = -\int_\Omega |\gamma \nabla u_\Omega|^2 \, dx,$$

under constraints on the surface measures of Γ_A and Γ_C.

Example: Optimization of a micro-osmotic mixer (II)

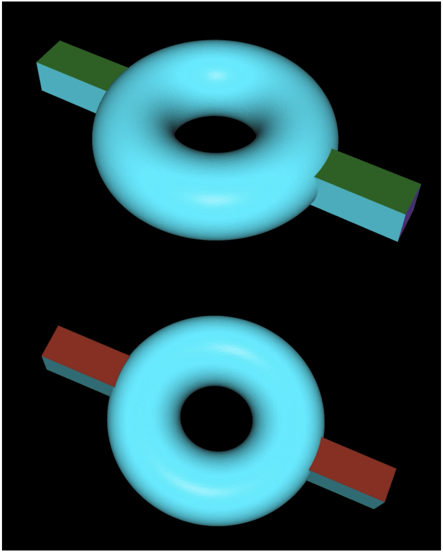

Optimization of (top) the anode, (bottom) the cathode of a micro-osmotic mixer.

An exotic notion of sensitivity with respect to the domain

Besides boundary perturbations and small holes, there is one third means to define "small" variations of Ω:

$$\Omega_{\sigma,\varepsilon} := \Omega \cup \omega_{\sigma,\varepsilon},$$

where

$$\omega_{\sigma,\varepsilon} := \left\{ x \in \mathbb{R}^d, \ \ d(x,\sigma) < \varepsilon \right\}$$

is a tube with thickness $\varepsilon \ll 1$ around a curve σ.

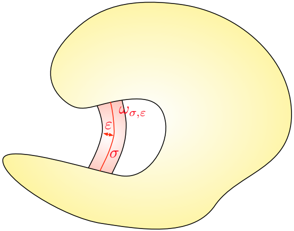

Such variations pave the way to a notion of topological ligament derivative:

$$J(\Omega_{\sigma,\varepsilon}) = J(\Omega) + \underbrace{\varepsilon^{d-1}}_{\approx|\omega_{\sigma,\varepsilon}|} \mathrm{d}J_L(\Omega)(\sigma) + \mathrm{o}(\varepsilon^{d-1}).$$

This topic has been seldom investigated in the literature. Unfortunately,

- The mathematical derivation of such asymptotic formulas is very difficult.
- The resulting expressions are difficult to use in practice.

S. Nazarov and J. Sokolowski, *The topological derivative of the dirichlet integral due to formation of a thin ligament*, Siberian Mathematical Journal, 45 (2004), pp. 341–355.

A model problem in linear elasticity

Background situation

The displacement $u_\Omega \in H^1(\Omega)^d$ is the solution to:

$$\begin{cases} -\mathrm{div}(Ae(u_\Omega)) = 0 & \text{in } \Omega, \\ u_\Omega = 0 & \text{on } \Gamma_D, \\ Ae(u_\Omega)n = g & \text{on } \Gamma_N, \\ Ae(u_\Omega)n = 0 & \text{on } \Gamma, \end{cases}$$

The performance of Ω equals $J(\Omega) = \int_\Omega j(u_\Omega)\,\mathrm{d}x$.

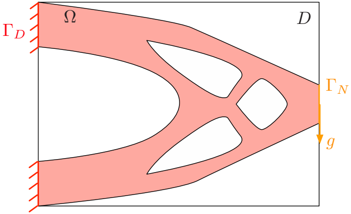

Perturbed situation

The perturbed displacement $u_\varepsilon \in H^1(\Omega_{\sigma,\varepsilon})^d$ satisfies:

$$\begin{cases} -\mathrm{div}(Ae(u_\varepsilon)) = 0 & \text{in } \Omega_{\sigma,\varepsilon}, \\ u_\varepsilon = 0 & \text{on } \Gamma_D, \\ Ae(u_\varepsilon)n = g & \text{on } \Gamma_N, \\ Ae(u_\varepsilon)n = 0 & \text{on } \Gamma \cup \partial\omega_{\sigma,\varepsilon}. \end{cases}$$

The performance of $\Omega_{\sigma,\varepsilon}$ reads $J(\varepsilon) := \int_{\Omega_{\sigma,\varepsilon}} j(u_\varepsilon)\,\mathrm{d}x$.

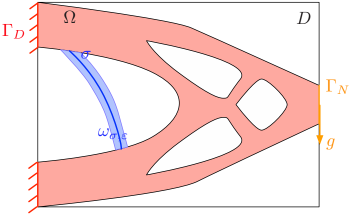

The general strategy to add a tube to a shape (I)

We approximate this setting by "filling the void" $D \setminus \overline{\Omega}$ with a soft material ηA, $\eta \ll 1$.

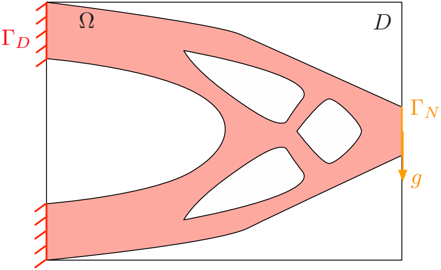

$\approx$

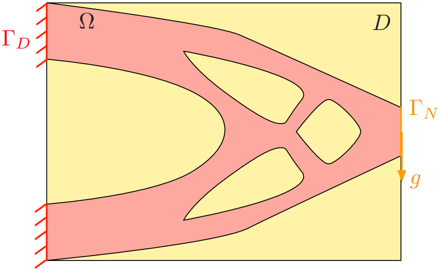

$$\begin{cases} -\mathrm{div}(Ae(u_\Omega)) = 0 & \text{in } \Omega, \\ u_\Omega = 0 & \text{on } \Gamma_D, \\ Ae(u_\Omega)n = g & \text{on } \Gamma_N, \\ Ae(u_\Omega)n = 0 & \text{on } \Gamma. \end{cases}$$

$$\begin{cases} -\mathrm{div}(A_\eta e(u_\eta)) = 0 & \text{in } D, \\ u_\eta = 0 & \text{on } \Gamma_D, \\ A_\eta e(u_\eta)n = g & \text{on } \Gamma_N, \\ A_\eta e(u_\eta)n = 0 & \text{on } \partial D \setminus (\overline{\Gamma_D} \cup \overline{\Gamma_N}), \end{cases}$$

$$A_\eta = \begin{cases} A & \text{if } x \in \Omega, \\ \eta A & \text{otherwise.} \end{cases}$$

We may as well use a smoothed Hooke's tensor A_η.

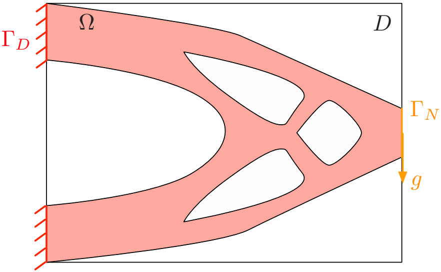

$\approx$

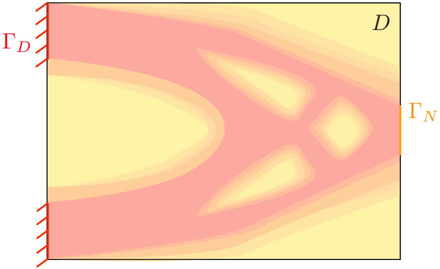

$$\begin{cases} -\mathrm{div}(Ae(u_\Omega)) = 0 & \text{in } \Omega, \\ u_\Omega = 0 & \text{on } \Gamma_D, \\ Ae(u_\Omega)n = g & \text{on } \Gamma_N, \\ Ae(u_\Omega)n = 0 & \text{on } \Gamma. \end{cases}$$

$$\begin{cases} -\mathrm{div}(A_\eta e(u_\eta)) = 0 & \text{in } D, \\ u_\eta = 0 & \text{on } \Gamma_D, \\ A_\eta e(u_\eta)n = g & \text{on } \Gamma_N, \\ A_\eta e(u_\eta)n = 0 & \text{on } \partial D \setminus (\overline{\Gamma_D} \cup \overline{\Gamma_N}), \end{cases}$$

$$A_\eta = (\text{smoothed}) \begin{cases} A & \text{if } x \in \Omega, \\ \eta A & \text{otherwise.} \end{cases}$$

We make a similar approximation for the perturbed problem.

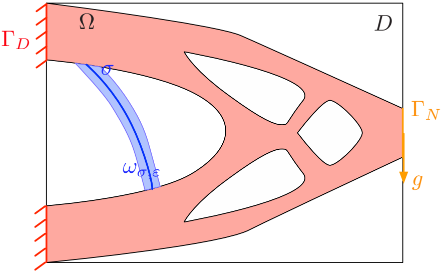

$\approx$

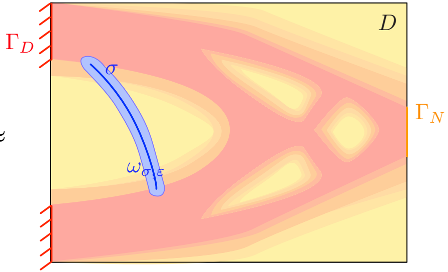

$$\begin{cases} -\mathrm{div}(Ae(u_\varepsilon)) = 0 & \text{in } \Omega_{\sigma,\varepsilon}, \\ u_\varepsilon = 0 & \text{on } \Gamma_D, \\ Ae(u_\varepsilon)n = g & \text{on } \Gamma_N, \\ Ae(u_\varepsilon)n = 0 & \text{on } \Gamma \cup \partial\omega_{\sigma,\varepsilon}. \end{cases}$$

$$\begin{cases} -\mathrm{div}(A_{\eta,\varepsilon}e(u_{\eta,\varepsilon})) = 0 & \text{in } D, \\ u_{\eta,\varepsilon} = 0 & \text{on } \Gamma_D, \\ A_{\eta,\varepsilon}e(u_{\eta,\varepsilon})n = g & \text{on } \Gamma_N, \\ A_{\eta,\varepsilon}e(u_{\eta,\varepsilon})n = 0 & \text{on } \partial D \setminus (\overline{\Gamma_D} \cup \overline{\Gamma_N}), \end{cases}$$

$$A_{\eta,\varepsilon} = \begin{cases} A & \text{if } x \in \omega_{\sigma,\varepsilon}, \\ A_\eta & \text{otherwise.} \end{cases}$$

The general strategy to add a tube to a shape (II)

- We make the formal approximations:

$$J(\Omega) \approx J(0) = \int_D j(u_\eta)\, \mathrm{d}x, \text{ and } J(\Omega_{\sigma,\varepsilon}) \approx J(\varepsilon) := \int_D j(u_{\eta,\varepsilon})\, \mathrm{d}x.$$

- The asymptotic behavior of $u_{\eta,\varepsilon}$ as $\varepsilon \to 0$ boils down to a problem of thin tubular inhomogeneities for the linear elasticity system.
- A (tedious) analysis yields:

$$u_{\eta,\varepsilon}(x) = u_\eta(x) + \varepsilon^{d-1} \int_\sigma \mathcal{M}(y) e(u_\eta) : e_y(N(x,y))\, \mathrm{d}\ell(y) + \mathrm{o}(\varepsilon^{d-1}),$$

and

$$J(\varepsilon) = J(0) - \varepsilon^{d-1} \int_\sigma \mathcal{M}(y) e(u_\eta) : e(p_\eta)\, \mathrm{d}\ell(y) + \mathrm{o}(\varepsilon^{d-1}),$$

where $\mathcal{M}(y)$ is a suitable polarization tensor and the adjoint state p_η satisfies:

$$\begin{cases} -\mathrm{div}(A_\eta e(p_\eta)) = -j'(u_\eta) & \text{in } D, \\ p_\eta = 0 & \text{on } \Gamma_D, \\ A_\eta e(p_\eta) n = 0 & \text{on } \partial D \setminus (\overline{\Gamma_D} \cup \overline{\Gamma_N}). \end{cases}$$

$\Rightarrow$ *The negativity of the first non trivial term indicates that it is beneficial to graft a thin tube based on σ to Ω.*

Application: Insertion of a bar in the course of a shape evolution (I)

- We minimize the compliance of a shape Ω under a volume constraint:

$$\min_{\Omega} J(\Omega) \text{ s.t. } \mathrm{Vol}\,(\Omega) \leq V_T,$$

$$\text{where } J(\Omega) := \int_{\Omega} Ae(u_{\Omega}) : e(u_{\Omega})\,\mathrm{d}x, \text{ and } \mathrm{Vol}(\Omega) = \int_{\Omega} \mathrm{d}x.$$

- The optimized shape is prone to falling into local minima with trivial topologies.

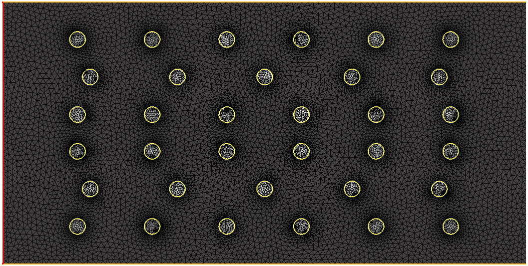

- To remedy this, we periodically interrupt the optimization process to insert bars.

Application: Insertion of a bar in the course of a shape evolution (II)

The "benchmark" 2d cantilever test case is considered.

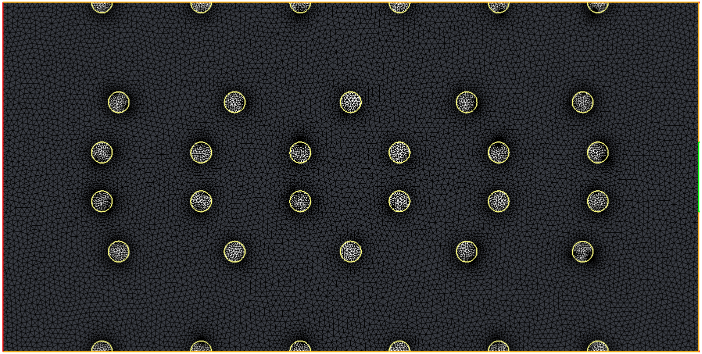

- The shape Ω is optimized with a boundary variation algorithm.
- Every now and then, the process in interrupted and a bar is added to Ω at an "optimal location".

Application: Insertion of a bar in the course of a shape evolution (III)

The optimization of a 3d bridge Ω is considered.

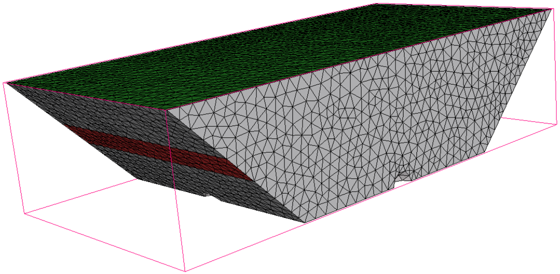

- We minimize the compliance of Ω

$$J(\Omega) = \int_\Omega Ae(u_\Omega) : e(u_\Omega)\,\mathrm{d}x.$$

- A volume constraint is enforced.
- Every now and then, a bar is added to Ω at an "optimal location".

Application: A "clever" initialization for truss structures (I)

- Truss structures are collections of bars.
- Many truss optimization methods rely on the ground structure approach: an initial, dense network of bars is iteratively decimated.
- We propose instead to start from void and
  1. Incrementally add bars to the structure.
  2. (Optionally) Take on the optimization with a more "classical" boundary-variation algorithm.

Example of a truss structure

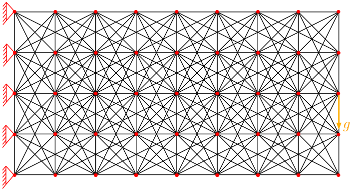

Initialization of a truss optimization algorithm by the ground structure approach

Application: A “clever” initialization for truss structures (II)

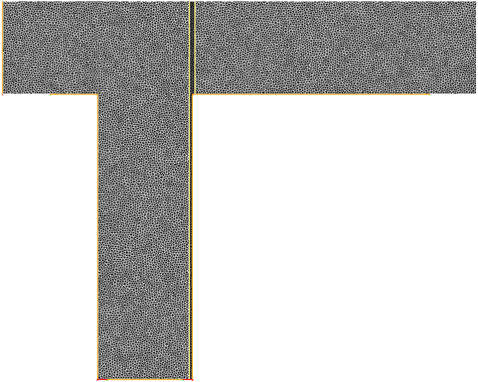

We consider the optimization of the shape of a 2d crane Ω.

- The compliance

  $$J(\Omega) := \int_\Omega Ae(u_\Omega) : e(u_\Omega)\,\mathrm{d}x$$

  is minimized.

- A volume constraint is enforced.

Evolution of shapes via Laguerre diagrams (I)

Ongoing work with B. Levy & E. Oudet

- The domain D is equipped with a Laguerre diagram:

$$\overline{D} = \bigcup_{i=1}^{N} \mathrm{Lag}_i(s,\psi), \text{ where } \begin{cases} s_1,\ldots,s_N \in D \text{ are seeds,} \\ \psi_1,\ldots,\psi_N \in \mathbb{R} \text{ are weights,} \end{cases}$$

and the i^{th} cell $\mathrm{Lag}_i(s,\psi)$ is defined by:

$$\mathrm{Lag}_i(s,\psi) = \left\{ x \in \overline{D}, |x-s_i|^2 - \psi_i \le |x-s_j|^2 - \psi_j, \forall j \neq i \right\}.$$

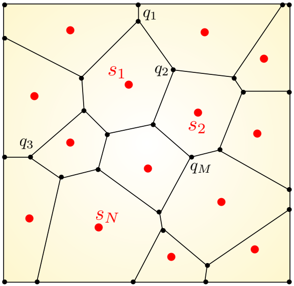

A Laguerre diagram of D

- The diagram can be parametrized by the seeds $s_1,\ldots,s_N$ and the measures $\nu_1,\ldots,\nu_N$ of the cells.
- This induces a decomposition of D into convex polygons, with vertices $q_1,\ldots,q_M$.
- The shape $\Omega \subset D$ is represented as a subdiagram:

$$\overline{\Omega} = \bigcup_{i=1}^{N_\Omega} \mathrm{Lag}_i(s,\psi).$$

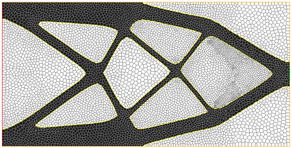

Representation of $\Omega \subset D$ as a subdiagram.

- We consider a shape optimization problem:

$$\min_{\Omega \subset D} J(\Omega) + (\text{constraints}),$$

where $J(\Omega)$ involves e.g. the elastic displacement u_Ω.

- The discretized version of this problem reads:

$$\min_{s,\, \nu} J(s, \nu).$$

- The mechanical calculations for u_Ω (and the adjoint p_Ω) hinge on the Virtual Element Method.

- This naturally yields the derivatives of J with respect to the vertices $q_1, \dots, q_M$ of the polygonal mesh.

- These derivatives are "transferred" at the seeds s and volumes ν by a suitable adjoint method.

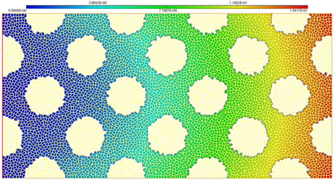

Virtual Element solution of the linear elasticity system.

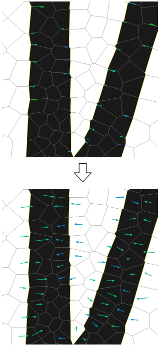

Sensitivity of J w.r.to vertices, then seed points.

Evolution of shapes via Laguerre diagrams (III): Numerical example

This framework is Lagrangian; yet, it naturally accounts for topological changes.

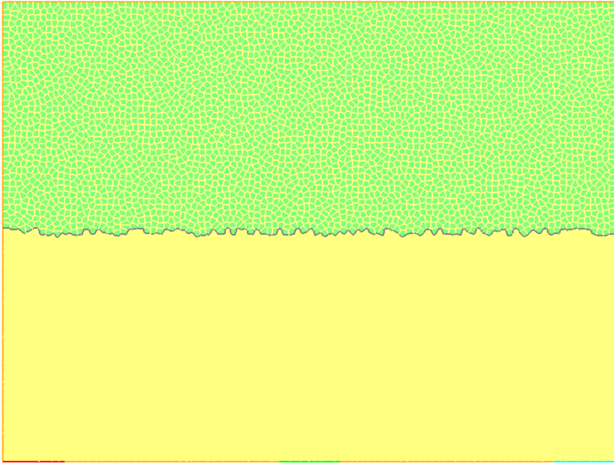

Thank you!

Further references I

[AlJak] G. Allaire, L. Jakabcin, *Taking into account thermal residual stresses in topology optimization of structures built by additive manufacturing*, Math. Models and Methods in Applied Sciences, 28(12), (2018), pp. 2313-2366.

[AmKa] H. Ammari and H. Kang, *Reconstruction of small inhomogeneities from boundary measurements*, Springer, 2004.

[Au] F. Aurenhammer, *Power diagrams: properties, algorithms and applications*, SIAM Journal on Computing, 16 (1987), pp. 78–96.

[BCGF] E. Beretta, Y. Capdeboscq, F. De Gournay, and E. Francini, *Thin cylindrical conductivity inclusions in a three-dimensional domain: a polarization tensor and unique determination from boundary data*, Inverse Problems, 25 (2009), p. 065004.

[BSCO] B. Boots, K. Sugihara, S. N. Chiu, and A. Okabe, *Spatial tessellations: concepts and applications of Voronoi diagrams*, John Wiley & Sons, 2009.

Further references II

[CGK] Y. Capdeboscq, R. Griesmaier, and M. Knöller, *An asymptotic representation formula for scattering by thin tubular structures and an application in inverse scattering*, Multiscale Modeling & Simulation, 19 (2021), pp. 846–885.

[CV] Y. Capdeboscq and M. S. Vogelius, *A general representation formula for boundary voltage perturbations caused by internal conductivity inhomogeneities of low volume fraction*, ESAIM: M2AN, 37 (2003), pp. 159–173.

[EsKu] P. Mohajerin Esfahani and D. Kuhn, *Data-driven distributionally robust optimization using the wasserstein metric: Performance guarantees and tractable reformulations*, Mathematical Programming, 171 (2018), pp. 115–166.

[FreSo] G. Fremiot and J. Sokolowski, *Shape sensitivity analysis of problems with singularities*, Lecture notes in pure and applied mathematics, (2001), pp. 255–276.

[GiRoStu] I. Gibson, D.W. Rosen and B. Stucker, *Additive manufacturing technology: rapid prototyping to direct digital manufacturing*, Springer Science Business Media, Inc, (2010).

[LaBa] J. J. Lang, M. Bastian, P. Foehr, M. Seebach, et al, *Improving mandibular reconstruction by using topology optimization, patient specific design and additive manufacturing?—A biomechanical comparison against miniplates on human specimen*. Plos one, 16(6),(2021), e0253002.

[PoFarCoMa] P. Pourabdollah, F. Farhang Mehr, S. Cockcroft and D. Maijer, *A new variant of the inherent strain method for the prediction of distortion in powder bed fusion additive manufacturing processes*, The International Journal of Advanced Manufacturing Technology, (2024), pp. 1–20.

[WeWuShi] Z. Wei, J. Wu, N. Shi et al, *Review of conformal cooling system design and additive manufacturing for injection molds*, Math. Biosci. Eng, 17(5), (2020), pp. 5414–5431.